CFD approach for two-phase CuO nanofluid flow through heat exchangers enhanced by double perforated louvered strip insert

M. E. Nakhchi[a], J. A. Esfahani[a,b,1]

[a] Department of Mechanical Engineering, Ferdowsi University of Mashhad, Mashhad 91775-1111, Iran

[b] Center of excellence on Modelling and Control Systems, (CEMCS), Ferdowsi University of Mashhad, Iran

Abstract

In this study, turbulent flow characteristics of CuO-water nanofluid through heat exchanger pipe enhanced with louvered strips are numerically investigated. Nanoparticles volume fraction (ϕ) varied from 0 to 2%. The louvered strips are mounted in single and double geometries. The slant angle(θ) and the Reynolds number (Re) are within $15^{\circ}-25^{\circ}$ and between 5,000 and 14,000, respectively. (RNG) $k-\epsilon$ model is employed based on the finite volume technique. The results illustrated that strong flow disturbance between the wall and the louvered strip is the main reason for turbulent kinetic energy increment. Besides, the nanoparticles improve the thermophysical properties of the working fluid, which results in better heat transfer. The Nu number increases 15.6% by using nanofluid instead of water at $\mathrm{Re}=14000$. The highest thermal enhancement parameter of 1.99 is obtained at $\mathrm{Re}=14000$ by using double perforated louvered strip with $\theta=25^{\circ}$. The recirculating flow inside the holes can significantly improve the thermal performance.

Keywords: Nanoparticles; Louvered strips; Turbulent flow; Heat transfer; CFD

[1] Corresponding author (abolfazl@um.ac.ir) Tel:+989150742484, https://orcid.org/0000-0001-6395-8089

1. Introduction

Performance enhancement is essential in the design of complex mechanical equipment such as heat exchanger tubes, solar collectors, process industry, and refrigeration. Different methods have been employed for thermal performance intensification of these systems by considering size and cost reductions. To this end, several passive methods are suggested by scientists to improve the thermal efficiency of mechanical structures in the past few years, like twisted tapes [1, 2], perforated turbulators [3, 4], hollow cylinders [5], conical rings [6, 7] and employing nanofluids [8-10] as the operating cooling fluid.

Using nanofluids can considerably improve the thermal performance and flow characteristics in many industrial thermal systems. Several researchers employed nanofluids with various kinds of nanoparticles (such as Cu [11], CuO [9], Ag [12], ZnO [13], etc.) to investigate the effects of nanoparticles volume fraction and other thermophysical parameters of nanoparticles on the performance augmentation of thermal equipment. Kefayati [14] numerically investigated the heat transfer and entropy generation of water with Cu nanoparticles inside a porous cavity. It was observed that increasing the volume fraction of nanoparticles significantly intensifies the heat transfer and entropy generation inside the cavity. The effects of Rayleigh number on the natural convection were also investigated. Nakhchi and Esfahani [7] investigated the impact of Cu-water nanofluid flow on the turbulent flow features of heat exchangers promoted by perforated conical rings. Their numerical simulation unveiled that the average Nusselt number could be augmented about 31.4% by raising the volume concentration of nanoparticles (ϕ) from 0 to 1.5%. In another numerical investigation, Selimefendigil and Oztop [15] evaluated the effects of CuO nanoparticles on mixed convection inside a 3D trapezoidal cavity with moving surfaces. It was deduced that the heat transfer augmentation of 25.3% could be reached by supplementing nanoparticles to the base fluid (water).

Using vortex generators are common in the design of heat exchanger tubes. They can significantly reduce the manufacturing costs of industrial thermal systems. Louvered strips are one of the most popular turbulators, which can substantially increase the thermal enhancement factor of heat exchangers by inducing additional vortex flows. These powerful vortex generators were firstly developed by Eiamsa-ard et al. [16]. In their analysis, typical louvered strips (LS) with several inclination angles were employed inside plain pipes, and the average Nusselt number and pressure drop were examined under turbulent flow regime. They used the louvered strips in forward and backward ways. It was concluded that the Nusselt number increases by about 284% compared to the plain tube by employing LS inserts with the highest slant angle (30^o). The experimental investigation of Yaningsih et al. [17] revealed that the performance of heat exchangers could considerably be improved by using forward LS inserts with different slant angles. They developed two equations for Nu number and pressure drop as functions of the thermophysical parameters. The results illustrated that LS inserts in the forward direction can improve the thermal enhancement factor up to 1.12. Fan et al. [18] performed a parametric study on the fluid flow characteristics inside tubes fitted with LS inserts. Their numerical simulations showed that the performance evaluation criterion (PEC) varied from 1.6 to 2.05. They also concluded that larger inclination angles and smaller pitch could intensify the Nusselt number inside heat exchanger tubes. Nakhchi et al.[19] numerically investigated the thermal characteristics and friction factor of turbulent water flow inside heat exchanger tubes fitted with perforated and typical louvered strip inserts in both single and double mounted conditions. The axial velocity contours, velocity vectors and temperature distributions were also investigated.

They reported that the thermal performance factor (η) could be increased up to 1.84 by using double perforation louvered strip (DPLS) turbulators. The additional recirculating flow near the holes was the most critical reason for heat transfer improvement in the existence of perforated turbulators.

The combined use of vortex generators and nanofluids is a powerful method for heat transfer promotion through heat exchangers and other thermal systems. Adding nanoparticles to the base fluids (water, ethylene glycol, etc.) can improve the thermophysical properties of the working fluid, which results in better heat transfer rates. Navaei et al. [20] numerically investigated the heat transfer and pressure loss inside channels with rib–groove turbulators. They employed four nanoparticle types (Al_2O_3, ZnO, CuO, and SiO_2) with various volume fractions. The Reynolds number was in the range of 5000-25,000. It was deduced that a semi-circular rib–groove turbulator with a height of 8 mm and pitch=48 mm results in the highest rate of heat transfer. Sundar and Sharma [21] experimentally examined the nanofluid flow characteristics inside a heat exchanger pipe equipped by twisted tape turbulators. They observed that using nanofluid with a volume concentration of 0.5% improves the heat transfer rate to 33.5% compared to water without nano additives. Vo et al. [22] performed a numerical simulation on heat transfer and pressure drop of γ-AlOOH nanofluid flow inside wavy channels. They used nano additives with five different shapes. It was concluded that platelet type nanoparticles improve the heat transfer rate better than the other test cases. Wongcharee and Eiamsa-Ard [23] applied CuO nanoparticles with water inside heat exchanger tubes enhanced by twisted tapes under the laminar flow regime. They reported that the Nusselt number is 13.8 times higher than that of pure water inside a circular pipe. In another numerical investigation, Mohammed et al. [24] employed nanofluids with four different nanoparticle types within heat exchanger pipes enhanced by louvered strip vortex generators. The numerical analysis showed that the forward LS insert can augment the average Nusselt number up to 411% at the highest inclination angle of $\alpha = 30°$.

The literature review illustrated that combined use of nanofluid with different nanoparticles and vortex generators can remarkably enhance the thermal performance of heat exchanger tubes. Employing louvered strip insert with different geometries and perforations is a novel method for heat transfer increment in various thermal systems. Based on the author's knowledge, there is no numerical or experimental investigation on nanofluid flow characteristics through heat exchangers promoted with perforated louvered strip turbulators under laminar or turbulent flow regimes. The advantages of these heat transfer intensification techniques motived us to investigate the thermal performance characteristics of CuO-water nanofluids flow inside heat exchanger tubes equipped with typical or perforated louvered strip vortex generators with various inclination angles and other geometrical parameters (single or double LS inserts). Then, the effects of nanoparticles volume fraction (ϕ) on the heat transfer rate, friction loss, and thermal enhancement parameter inside the tubes promoted by SPLS and DPLS turbulators are also investigated.

2. Physical description

The geometrical parameters of the heat exchanger tube fitted with the perforated louvered strip (PLS) insert are presented in Fig.1. The tube is circular, and CuO-water nanofluid with the inlet temperature of 300K and uniform velocity moves inside the pipe. The tube length (L=2210mm) and the diameter of the tube (D=14.3mm) are kept constant in this study. The pipe is enhanced with PLS inserts, which are attached to the connecting rod with a specific inclination angle (θ).

The inclination angle varied from 15^{o} to 25^{o} in the present numerical simulations. Five holes are created on the louvered strips at equal distances. The schematic view shows that the perforated louvered strips are elliptical $\left(6\times10mm\right)$. Besides, they are mounted in a single (SPLS) and double (DPLS) positions on the connecting rod. The diameter of the connecting rod (δ) and the thickness of the PLS inserts (t) are 1mm. To compare the influence of the holes on the thermal performance of the perforated louvered strip inserts, the numerical simulations are validated with the conventional (non-perforated) strip inserts with varying slant angles. The volume concentration of CuO nanoparticles (ϕ) changed from 0 (pure water) to 2%. Also, the physical parameters of the nanofluid are selected based on empirical correlations.

The temperature of the tube wall (T_w) is assumed to be constant at 333K to make validation with the experimental results of Yaningsih [17] for conventional louvered strips. The inlet velocity (u_{in}) is uniform and the Reynolds number as a function of the inlet velocity $\left(\mathrm{Re}=u_{in}D/\nu\right)$ is in the range of 5000 to 14000 and the nanofluid flow is turbulent. The PLS inserts are assumed to be adiabatic, and the mixture model is used for simulation of nanofluid flow. No-slip boundary condition is imposed on the tube walls.

3. Computational analysis

The governing equations (continuity, momentum, and energy) for steady, incompressible and three-dimensional flows based on RANS model are as follows:

$$\frac{\partial}{\partial x_i}(\rho u_i)=0 \tag{1}$$

$$\frac{\partial}{\partial x_j}\left(u_j \rho u_i\right)=\frac{\partial}{\partial x_j}\left[-\rho\overline{u_i{}'u_j{}'}\right]-\frac{\partial p}{\partial x_i}+\frac{\partial}{\partial x_j}\left\{\mu\left[\frac{\partial u_i}{\partial x_j}+\frac{\partial u_j}{\partial x_i}\right]\right\} \tag{2}$$

$$\frac{\partial}{\partial x_j}\left(\rho T u_i\right)=\frac{\partial}{\partial x_i}\left\{\frac{\partial T}{\partial x_i}\left[\frac{\mu}{\mathrm{Pr}}+\frac{\mu_t}{\mathrm{Pr}_t}\right]\right\} \tag{3}$$

where ρ , u, p, T, μ, Pr and Pr_t are fluid density, nanofluid velocity, pressure, temperature, dynamic viscosity, Prandtl number, and turbulent Prandtl number, respectively. $\mu_t=\rho C_\mu \frac{k^2}{\epsilon}$ is the turbulent viscosity and $\rho\overline{u_i{}'u_j{}'}$ is defined as [2]:

$$-\rho\overline{u_i{}'u_j{}'}=\mu_t\left[\frac{\partial u_i}{\partial x_j}+\frac{\partial u_j}{\partial x_i}\right]-\frac{2}{3}\mu_t\frac{\partial u_k}{\partial x_k}\delta_{ij}-\frac{2}{3}\rho k\,\delta_{ij} \tag{4}$$

k and ε equations based on the turbulent model are defined as [25]:

$$\frac{\partial}{\partial x_i}\left(\rho u_i k\right)=\frac{\partial}{\partial x_j}\left\{\left[\frac{\mu_t}{\sigma_k}+\mu\right]\frac{\partial k}{\partial x_j}\right\}-\rho\varepsilon+G_k \tag{5}$$

$$\frac{\partial}{\partial x_i}\left(\rho u_i \varepsilon\right)=\frac{\partial}{\partial x_j}\left\{\left[\frac{\mu_t}{\sigma_\varepsilon}+\mu\right]\frac{\partial \varepsilon}{\partial x_j}\right\}+\frac{\varepsilon}{k}\left[C_{1\varepsilon}G_k-\rho C_{2\varepsilon}\varepsilon\right] \tag{6}$$

where $G_k=-\rho\overline{u_i{}'u_j{}'}\frac{\partial u_j}{\partial x_i}$ and the constants used in the above equations are selected to be: $C_{1\varepsilon}=1.42, \mathrm{Pr}_t=0.85, C_\mu=0.084, C_{2\varepsilon}=1.68, \sigma_k=1$ and $\sigma_\varepsilon=1.3$.

Ansys ICEM 19.1 is employed for mesh generation through the heat exchanger. As depicted in Fig. 2, the tetrahedral mesh is applied inside the tube, while prism mesh with ten inflation layers with an enhancement rate of 1.1 is used near the tube walls to detect the turbulent viscous sub-layer effects. As can be seen, a finer mesh is generated near the PLS turbulators to predict better the vortex generation of nanofluid flow in these areas. The maximum element size was assumed to be less than 0.1mm in the computational domain. y^+ values near the pipe surface were smaller than 1 in the whole finite volume simulations.

Various RANS turbulent models, including standard k-ε, (RNG) k-ε, $k-\omega$ and SST $k-\omega$ were employed in the present study. After validation with the experimental results (See Fig. 4), it was observed that the RNG k-ε model performed better than the other models. Therefore, it was selected for further simulations. This model is able to predict the recirculation flows near the holes of the vortex generators.

The main dimensionless physical parameters for measuring the performance of heat exchangers, Reynolds number, Nusselt number, friction factor (f), and the thermal performance factor (η), can be expressed as [26]:

$$\mathrm{Re} = \frac{u_i D}{\nu} \tag{7}$$

$$Nu = \frac{hD}{k} \tag{8}$$

$$f = \frac{2D}{L}\frac{\Delta P}{\rho u^2} \tag{9}$$

$$\eta = \frac{\left(Nu / Nu_p\right)}{\left(f / f_p\right)^{1/3}} \tag{10}$$

In the above equations, u_i is the axial nanofluid velocity, D is the tube diameter, ν is the kinematic viscosity, and k is assumed to be the thermal conductivity of the fluid, respectively. Nu_p and f_p are specified as the heat transfer coefficient and friction loss of nanofluid flows in the plain pipe, respectively. The main physical properties of Cuo-H_2O nanofluid, including density (ρ_{eff}), specific heat (C_{eff}), and viscosity (μ_{eff}) for nanoparticle volume fractions varying from 0 (pure water) to 2% could be calculated by employing these equations [26, 27]:

$$\rho_{eff} = (1-\phi)\rho_f + \phi\rho_p \tag{11}$$

$$C_{eff} = \frac{(1-\phi)\rho_f C_f + \phi\rho_p C_p}{\rho_{eff}} \tag{12}$$

$$\mu_{eff} = \frac{\mu_f}{(1-\phi)^{2.5}} \tag{13}$$

where ϕ, f, and p are volume fraction of nanoparticles, base fluid, and CuO nanoparticles, respectively. The Thermal conductivity of nanofluid can also be evaluated by [28]:

$$\frac{k_{eff}}{k_f} = \frac{k_p + 2k_f + 2\phi(k_p - k_f)}{k_p + 2k_f - \phi(k_p - k_f)} \tag{14}$$

The thermophysical properties of CuO nanoparticles are selected as $C_p = 540 J/kg.K$, $\rho_p = 6500 kg/m^3$ and $k_p = 18\ W/m.K$.

Fig. 3 illustrates the grid independency check for the heat exchangers promoted by double perforated louvered strips with $\theta = 25^{\circ}$ at the Reynolds number of 14000. The nanoparticles volume concentration is kept constant at 1.5%. The friction factor coefficient and Nu number are employed to check the grid independence. As can be seen, the variations between 2,566,207 and 5,122,678 elements for both of Nu and f parameters are small and negligible. Thus 2,566,207 grid number is used for further analysis. Similar grid studies are also performed for all of the test cases in the present numerical simulations.

Fig. 4 shows the validity of CFD simulations with the experimental data of Yaningsih [17] for turbulent flow inside the circular tube fitted with typical louvered strip insert with two different inclination angles $\left(\theta = 15^{\circ} \text{and } 25^{\circ}\right)$. The working fluid is water $\left(\phi = 0\right)$ and two comparisons are made for an average Nu number and friction loss for various Reynolds numbers. It can be seen that the numerical simulations are following the experimental results. This validation shows that the grid generation and the solution algorithm are accurate. Thus, further simulations can be performed for other types of PLS and DPLS inserts.

In order to show the accuracy of nanofluid flow simulations, additional validations are performed to compare with the experimental results. Table 1 shows a comparison between the numerical results of the present study for average Nusselt number and experimental data of Naik et al. [29] for turbulent CuO-water nanofluid flow inside tubes without inserts at two different nanoparticles volume fractions. It can be seen that the numerical results are in agreement with experimental data.

4. Results and discussions

Fig. 5 illustrates the streamlines of nanofluids flow in a smooth tube and the tubes equipped by perforated louvered strips with different geometries as functions of turbulent kinetic energy (TKE). The Reynolds number is kept constant at 5,000 and the nanoparticle volume fraction $\left(\phi\right)$ is assumed to be 1%. Overall, it can be seen that by employing PLS and DPLS inserts, the TKE increases in the axial direction, while it remains constant inside the plain tube. The results show that TKE is considerably augmented by raising the inclination angle from 15$^{\text{o}}$ to 25$^{\text{o}}$. The main physical reason for the TKE enhancement is stronger vortex flows near the DPLS insert with $\theta = 25^{\circ}$. It also can be seen that the flow perturbation is significantly increased by using DPLS insert with higher inclination angles. The flow perturbation improves the fluid combination between the heat exchanger center and the walls, which intensifies the heat transfer rate.

Fig. 6 shows the surface streamlines of turbulent CuO-water nanofluid flow with the nanoparticles volume fraction of $\phi = 1\%$ inside heat exchanger tubes fitted with SPLS and DPLS turbulators at z=113mm. Streamlines show the tangent to the velocity vector of the flow in this cross section. The streamlines illustrate that for all of the cases, the turbulent kinetic energy is higher near the perforations of the louvered strips. This is mostly because of the more energetic flow within the holes and the recirculating flows between the core region and the pipe surface. It can be seen that the TKE is considerably increased with rising the slant angles from 15^{o} to 25^{o}. The main physical reason for TKE enhancement is further vortex flows generated near the perforations of the louvered strips with higher slant angles. Moreover, the passing fluid within the perforations increases the fluid mixing, which promotes the heat transfer in the heat exchanger tube.

Fig. 7 displays the axial velocity contour of CuO-water nanofluid flows within the pipes supported by perforated louvered strips at three different cross-sections. The results indicate that the axial velocity of turbulent nanofluid flow for the case of DPLS insert is more effective than the others. This strong axial velocity disrupts the thermal boundary layer near the tube surface and augments the heat transfer rate. The axial flows in the backward direction $\left(-0.1 < u < 0\right) m/s$ is generated near the perforations of PLS inserts. The backward flow is due to the recirculation flow near the apertures. It can be seen that the axial velocity at section ‘A’ is higher than the other cross-sections for all of the test cases. This is because of the jet generation between the louvered strips and the pipe surface which is formed based on the conservation of mass flow rate.

The 2D axial velocity streamlines of nanofluid flow within the heat exchanger pipe fitted by typical louvered strip (LS) and DLPS inserts with $\theta = 25^{\circ}$ in the X-Z plane are presented in Fig. 8. The nanoparticles volume fraction is kept constant at 1%, and the Reynolds number is 5,000. The primary and secondary vortex flows near the perforations can be observed for the case of DPLS insert. The extra eddy flows adjacent to the holes, significantly increase the flow disturbance and perturbations of turbulent nanofluid flow within the heat exchangers pipes. This additional flow disturbance considerably increases the friction loss and fluid mixing between the core and the pipe surface. The jet formation near tube walls is the essential physical cause for the thermal boundary-layer perturbation near of perforated louvered strips.

Fig. 9 displays the effects of nanoparticles volume fraction (ϕ) on the temperature distribution of the fluid flow in X-Y plane inside the tubes promoted with SPLS and DPLS turbulators with $\theta = 25^{\circ}$. The CuO nanoparticles volume fraction is varied from 0 (pure water) to 1.5%. It can be observed that the temperature of the nanofluid is increased by increasing the nanoparticles volume concentration. This is mainly because of the enhanced physical properties of the nanofluids (thermal conductivity, specific heat, and viscosity) compared to pure water. It also can be seen that the temperature distribution of nanofluid flow through the tube fitted with DPLS insert is generally higher than that with SPLS inserts. The main reason for this augmentation is additional vortex flows generated near the DPLS turbulators in comparison with SPLS inserts.

Fig. 10 illustrates the influences of louvered strips with different geometries on the temperature contours of nanofluid flow inside the circular tubes at three different axial locations. The Reynolds number is uniform (Re=5,000) for all of the simulations. The results show that the temperature enhancement for the case of DPLS insert with $\theta = 25^{\circ}$ is higher than the other tested geometries. As discussed earlier, the jet generation close to the pipe surface and the DPLS and the additional recirculation flow between the perforations are the essential physical causes for heat transfer improvement in the presence of DPLS insert with higher slant angles. The primary vortex flows inside the apertures of the DPLS intensifies the turbulent kinetic energy in that region. Thus, fluid reattachment between the core of the pipe and the walls is increased. The results illustrate that the temperature of nanofluid increases by raising the inclination angle from 15^{o} to 25^{o} because of the more robust jet flow near the pipe surface. It is also clear the temperature enhancement for perforated louvered strip inserts is generally higher than that for typical louvered strips without perforations.

Fig. 11 shows the trend of the Nu number to the Re number for heat exchangers promoted with louvered strip turbulators with and without perforations. The effects of the slant angle on the heat transfer coefficient are also presented. The volume concentration of CuO nanoparticles is kept constant at 1%. As expected, the heat transfer rate enhances with the Re number, which is due to stronger temperature gradients near the walls. It can be seen that the heat transfer rate for the case of DPLS insert is the highest between various louvered strip inserts. The average Nusselt number increment is the result of the extra recirculating flow inside the perforations of the DPLS inserts. It also should be pointed out the primary vortex flows and the nanofluid flow attachment are the other main physical parameters describing the heat transfer augmentation for the heat exchanger tube equipped with DPLS insert. It can be observed that the average Nu number is increased by increasing the inclination angles from 15 to 25 degrees. This is mostly because of the stronger jet generation close to the walls of the heat exchanger pipes promoted by louvered strip turbulators with higher inclination angles. It can be concluded that the average Nu number for the case of DPLS inserts with $\theta = 25^\circ$ is 60.1%, 45.8%, and 26.8%, respectively higher than LS, SPLS, and DLS vortex generators with similar slant angles.

Fig. 12 depicts the effects of CuO nanoparticle volume concentration (ϕ) on the average heat transfer coefficient in the heat exchanger tube promoted by DPLS insert with $\theta = 25^\circ$. The chart shows that the Nu number increases by about 15.6% by using CuO nanofluid instead of pure water at Re=14000. The trend of Nu variations with ϕ is nearly similar for all of the axial inlet velocities. However, heat transfer augmentation at higher Reynolds number is slightly better compared to the lower Re numbers. The main physical reason for heat transfer augmentation in the presence of nanoparticles is improved thermophysical properties of nanofluid compared to pure water. Another substantial reason for Nu number enhancement is the Brownian motions between the CuO nanoparticles.

Fig. 13 illustrates the impact of different louvered strip inserts on the friction loss of CuO-water nanofluid flow in a heat exchanger pipe for two different inclination angles $\left(\theta = 15^\circ, 25^\circ\right)$. The nanoparticles volume fraction is kept constant at 1%. Overall, it can be deduced that the friction factor fells by raising the Re number. The trend of the variations is similar to the Moody chart for turbulent fluid flows. In detail, the friction loss of nanofluids flow inside the pipes promoted by louvered strips considerably increases compared to the plain tube without an insert. It is maximum for the case of DPLS insert. It also can be seen that the friction coefficient significantly intensifies by the slant angle (θ). This augmentation is mostly because of the additional vortex flows in the presence of louvered strip inserts with higher slant angles. As discussed earlier, perforations increase the disturbance and flow perturbations near the PLS and DPLS inserts. This is the primary physical reason for higher friction loss for DPLS insert in comparison with typical LS and DLS inserts. The highest friction factor (f=0.171) is reached by employing DPLS turbulators with $\theta = 25^{\circ}$ at Re=5000. The friction factor of nanofluids flows inside heat exchanger pipes enhanced by LS, SPLS and DPLS turbulators with the inclination angle of 15^{o} are 58.8%, 64.7%, and 73.5%, respectively higher than that of the simple plain tube with similar Reynolds numbers.

Fig. 14 shows the effects of CuO nanoparticle volume fraction (ϕ) on the friction factor of turbulent nanofluid flow in heat exchanger pipes equipped with the double perforated louvered strip (DPLS) inserts with an inclination angle of 25^{o}. It can be observed that the friction parameter promotes by raising ϕ from 0 (pure water) to 2%. This augmentation is because of improved viscosity of nanofluid in comparison with water without any nanoparticles. The CuO nanoparticle interaction increases the wall shear rate. Using nanofluids with $\phi = 0.5\%$, 1%, 1.5% and 2% increases the friction factor about 4.7%, 7.8%, 10.2% and 14.1%, respectively compared to pure water.

The effects of various louvered strip inserts with different slant angles on the thermal performance factor of CuO-water nanofluid flow inside a heat exchanger pipe with $\phi = 2\%$ are depicted in Fig. 15. It can be deduced that all of the PLS and DPLS turbulators perform better than the conventional LS inserts (Yaningsih et al. [17]) with the same slant angle. Moreover, the slant angle increment from 15^{o} to 25^{o} significantly increases the thermal performance factor. The recirculating flow inside the holes along with the flow disturbance between the louvered strips and the tube walls, which disrupt the thermal boundary layer, are the main physical parameters for performance intensification. In addition, the highest thermal enhancement parameter of 1.99 is obtained at Re=14,000 by using DPLS insert with $\theta = 25^{\circ}$.

Fig. 16 shows a comparison between the thermal performance obtained in the present study and the other recent numerical and experimental studies in the field of vortex generators and turbulators. It can be seen that the thermal performance of nanofluid flow inside heat exchanger tubes fitted by DPLS insets performs better than the other vortex generators when Re>8000. The comparison shows that combined use of nanofluids and double perforated louvered strips with the slant angle of $\theta = 25^{\circ}$ with nanoparticles volume fraction of 2% is an excellent choice to improve the performance of the heat exchangers.

5. Conclusion

In this study, the combined effects of CuO-water nanofluids and perforated louvered strip vortex generators with various geometries on the turbulent flow characteristics inside circular tubes were numerically investigated. The nanoparticles volume concentration was between 0 and 2%, and the Reynolds number varied from 5,000 to 14000. The flow streamlines, axial velocity contours and vectors, turbulent kinetic energy and temperature contours and thermal-hydraulic performance parameters were also investigated. The main achievements in the present study can be summarized as:

- Turbulent kinetic energy is considerably augmented by raising the slant angle from 15° to 25°. The main physical reasons for the TKE enhancement are stronger vortex flows near the DPLS insert and additional recirculating flow within the holes of the louvered strip turbulators with $\theta = 25^{\circ}$.

- The chart shows that the Nu number increases by 15.6% by using CuO nanofluid instead of pure water at Re=14000.
- The friction loss of nanofluids flow inside the heat exchanger pipe augmented by LS, SPLS and DPLS turbulators with the inclination angle of 15^{o} are 58.8%, 64.7% and 73.5%, respectively higher than that of the simple plain tube with similar Reynolds numbers.
- Using DPLS inserts and nanofluids with CuO nano additives with $\phi = 0.5\%$, 1%, 1.5% and 2% increase the friction factor about 4.7%, 7.8%, 10.2% and 14.1%, respectively compared to pure water.
- The highest friction factor (f=0.171) could be obtained by employing DPLS turbulators with $\theta = 25^{\circ}$ at Re=5000.
- The maximum thermal enhancement parameter of 1.99 is obtained at Re=14,000 by using DPLS insert with $\theta = 25^{\circ}$. The recirculating flow inside the holes and the flow disturbance between the louvered strips and the tube walls which disrupt the thermal boundary layer are the main physical parameters for the performance improvement.

Acknowledgement

This research is financially supported by the Ferdowsi University of Mashhad under contract No. 51059.

References

[1] M. Nakhchi, J. Esfahani, Cu-water nanofluid flow and heat transfer in a heat exchanger tube equipped with cross-cut twisted tape, Powder Technology, 339 (2018) 985-994.

[2] M. Nakhchi, J. Esfahani, Numerical investigation of rectangular-cut twisted tape insert on performance improvement of heat exchangers, International Journal of Thermal Sciences, 138 (2019) 75-83.

[3] V. Kongkaitpaiboon, K. Nanan, S. Eiamsa-Ard, Experimental investigation of heat transfer and turbulent flow friction in a tube fitted with perforated conical-rings, International Communications in Heat and Mass Transfer, 37(5) (2010) 560-567.

[4] S. Chingulpitak, H.S. Ahn, L.G. Asirvatham, S. Wongwises, Fluid flow and heat transfer characteristics of heat sinks with laterally perforated plate fins, International Journal of Heat and Mass Transfer, 138 (2019) 293-303.

[5] M. Nakhchi, J. Esfahani, Numerical investigation of heat transfer enhancement inside heat exchanger tubes fitted with perforated hollow cylinders, International Journal of Thermal Sciences, 147 (2020) 106153.

[6] M. Nakhchi, J. Esfahani, Numerical investigation of different geometrical parameters of perforated conical rings on flow structure and heat transfer in heat exchangers, Applied Thermal Engineering, 156 (2019) 494-505.

[7] M. Nakhchi, J. Esfahani, Numerical investigation of turbulent Cu-water nanofluid in heat exchanger tube equipped with perforated conical rings, Advanced Powder Technology, 30(7) (2019) 1338-1347.

[8] K.M. Shirvan, M. Mamourian, S. Mirzakhanlari, R. Ellahi, Numerical investigation of heat exchanger effectiveness in a double pipe heat exchanger filled with nanofluid: a sensitivity analysis by response surface methodology, Powder Technology, 313 (2017) 99-111.

[9] M. Jafaryar, M. Sheikholeslami, Z. Li, CuO-water nanofluid flow and heat transfer in a heat exchanger tube with twisted tape turbulator, Powder technology, 336 (2018) 131-143.

[10] R. Ellahi, A. Zeeshan, N. Shehzad, S.Z. Alamri, Structural impact of kerosene-Al 2 O 3 nanoliquid on MHD Poiseuille flow with variable thermal conductivity: Application of cooling process, Journal of Molecular Liquids, (2018).

[11] N. Biswas, N.K. Manna, P. Datta, P.S. Mahapatra, Analysis of heat transfer and pumping power for bottom-heated porous cavity saturated with Cu-water nanofluid, Powder technology, 326 (2018) 356-369.

[12] E. Khodabandeh, M. Bahiraei, R. Mashayekhi, B. Talebjedi, D. Toghraie, Thermal performance of Ag–water nanofluid in tube equipped with novel conical strip inserts using two-phase method: Geometry effects and particle migration considerations, Powder technology, 338 (2018) 87-100.

[13] L. Huaxu, W. Fuqiang, L. Dong, Z. Jie, T. Jianyu, Optical properties and transmittances of ZnO-containing nanofluids in spectral splitting photovoltaic/thermal systems, International Journal of Heat and Mass Transfer, 128 (2019) 668-678.

[14] G. Kefayati, Heat transfer and entropy generation of natural convection on non-Newtonian nanofluids in a porous cavity, Powder technology, 299 (2016) 127-149.

[15] F. Selimefendigil, H.F. Öztop, A.J. Chamkha, Analysis of mixed convection of nanofluid in a 3D lid-driven trapezoidal cavity with flexible side surfaces and inner cylinder, International Communications in Heat and Mass Transfer, 87 (2017) 40-51.

[16] S. Eiamsa-ard, S. Pethkool, C. Thianpong, P. Promvonge, Turbulent flow heat transfer and pressure loss in a double pipe heat exchanger with louvered strip inserts, International Communications in Heat and Mass Transfer, 35(2) (2008) 120-129.

[17] I. Yaningsih, A.T. Wijayanta, T. Miyazaki, S. Koyama, Thermal hydraulic characteristics of turbulent single-phase flow in an enhanced tube using louvered strip insert with various slant angles, International Journal of Thermal Sciences, 134 (2018) 355-362.

[18] A. Fan, J. Deng, A. Nakayama, W. Liu, Parametric study on turbulent heat transfer and flow characteristics in a circular tube fitted with louvered strip inserts, International Journal of Heat and Mass Transfer, 55(19-20) (2012) 5205-5213.

[19] M. Nakhchi, J. Esfahani, K. Kim, Numerical study of turbulent flow inside heat exchangers using perforated louvered strip inserts, International Journal of Heat and Mass Transfer, 148 (2020) 119143.

[20] A. Navaei, H. Mohammed, K. Munisamy, H. Yarmand, S. Gharehkhani, Heat transfer enhancement of turbulent nanofluid flow over various types of internally corrugated channels, Powder technology, 286 (2015) 332-341.

[21] L.S. Sundar, K. Sharma, Turbulent heat transfer and friction factor of Al2O3 nanofluid in circular tube with twisted tape inserts, International Journal of Heat and Mass Transfer, 53(7-8) (2010) 1409-1416.

[22] D.D. Vo, J. Alsarraf, A. Moradikazerouni, M. Afrand, H. Salehipour, C. Qi, Numerical investigation of γ-AlOOH nano-fluid convection performance in a wavy channel considering various shapes of nanoadditives, Powder technology, 345 (2019) 649-657.

[23] K. Wongcharee, S. Eiamsa-Ard, Enhancement of heat transfer using CuO/water nanofluid and twisted tape with alternate axis, International Communications in Heat and Mass Transfer, 38(6) (2011) 742-748.

[24] H. Mohammed, H.A. Hasan, M. Wahid, Heat transfer enhancement of nanofluids in a double pipe heat exchanger with louvered strip inserts, International Communications in Heat and Mass Transfer, 40 (2013) 36-46.

[25] M.E. Nakhchi, J. Esfahani, Sensitivity analysis of a heat exchanger tube fitted with cross-cut twisted tape with alternate axis, Journal of Heat Transfer, 141(4) (2019) 041902.

[26] M. Nakhchi, J. Esfahani, Numerical investigation of turbulent Cu-water nanofluid in heat exchanger tube equipped with perforated conical rings, Advanced Powder Technology, (2019).

[27] M. Rajarathinam, N. Nithyadevi, A.J. Chamkha, Heat transfer enhancement of mixed convection in an inclined porous cavity using Cu-water nanofluid, Advanced Powder Technology, 29(3) (2018) 590-605.

[28] J.C. Maxwell, J.J. Thompson, A treatise on electricity and magnetism, Clarendon, 1904.

[29] M. Naik, S.S. Fahad, L.S. Sundar, M.K. Singh, Comparative study on thermal performance of twisted tape and wire coil inserts in turbulent flow using CuO/water nanofluid, Experimental Thermal and Fluid Science, 57 (2014) 65-76.

[30] S. Eiamsa-Ard, P. Somkleang, C. Nuntadusit, C. Thianpong, Heat transfer enhancement in tube by inserting uniform/non-uniform twisted-tapes with alternate axes: Effect of rotated-axis length, Applied Thermal Engineering, 54(1) (2013) 289-309.

[31] M. Rahimi, S.R. Shabanian, A.A. Alsairafi, Experimental and CFD studies on heat transfer and friction factor characteristics of a tube equipped with modified twisted tape inserts, Chemical Engineering and Processing: Process Intensification, 48(3) (2009) 762-770.

[32] S. Eiamsa-Ard, P. Promvonge, Performance assessment in a heat exchanger tube with alternate clockwise and counter-clockwise twisted-tape inserts, International Journal of Heat and Mass Transfer, 53(7-8) (2010) 1364-1372.

[33] S. Eiamsa-ard, P. Seemawute, K. Wongcharee, Influences of peripherally-cut twisted tape insert on heat transfer and thermal performance characteristics in laminar and turbulent tube flows, Experimental Thermal and Fluid Science, 34(6) (2010) 711-719.

[34] P. Murugesan, K. Mayilsamy, S. Suresh, Turbulent heat transfer and pressure drop in tube fitted with square-cut twisted tape, Chinese Journal of Chemical Engineering, 18(4) (2010) 609-617.

[35] S. Eiamsa-Ard, C. Thianpong, P. Eiamsa-Ard, Turbulent heat transfer enhancement by counter/co-swirling flow in a tube fitted with twin twisted tapes, Experimental Thermal and Fluid Science, 34(1) (2010) 53-62.

[36] A. Saysroy, W. Changcharoen, S. Eiamsa-ard, Performance assessment of turbular heat exchanger tubes containing rectangular-cut twisted tapes with alternate axes, Journal of Mechanical Science and Technology, 32(1) (2018) 433-445.

[37] N. Piriyarungrod, M. Kumar, C. Thianpong, M. Pimsarn, V. Chuwattanakul, S. Eiamsa-ard, Intensification of thermo-hydraulic performance in heat exchanger tube inserted with multiple twisted-tapes, Applied Thermal Engineering, 136 (2018) 516-530.

[38] P. Promvonge, S. Skullong, Thermo-hydraulic performance in heat exchanger tube with V-shaped winglet vortex generator, Applied Thermal Engineering, 164 (2020) 114424.

[39] W. Chingtuaythong, P. Promvonge, C. Thianpong, M. Pimsarn, Heat transfer characterization in a tubular heat exchanger with V-shaped rings, Applied Thermal Engineering, 110 (2017) 1164-1171.

[40] P. Promvonge, Thermal augmentation in circular tube with twisted tape and wire coil turbulators, Energy Conversion and Management, 49(11) (2008) 2949-2955.

List of Figures

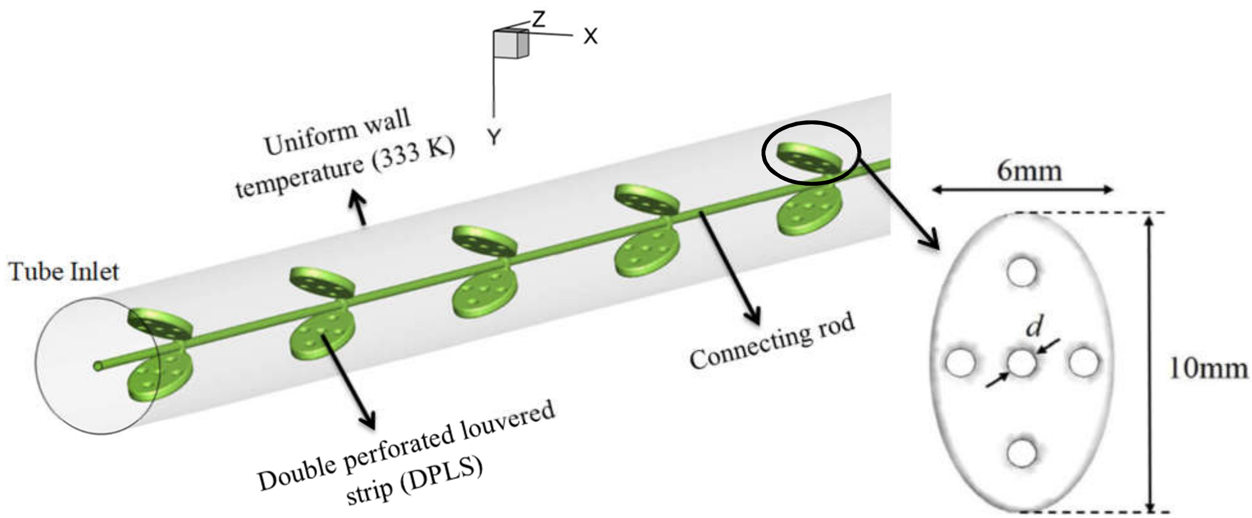

a) Three dimensional view

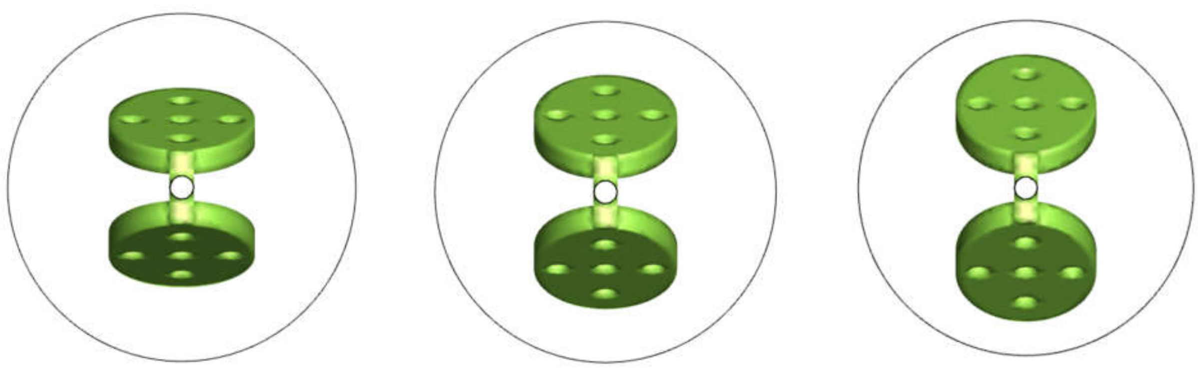

PLS $\left(\theta = 15^{\circ}\right)$ PLS $\left(\theta = 20^{\circ}\right)$ PLS $\left(\theta = 25^{\circ}\right)$

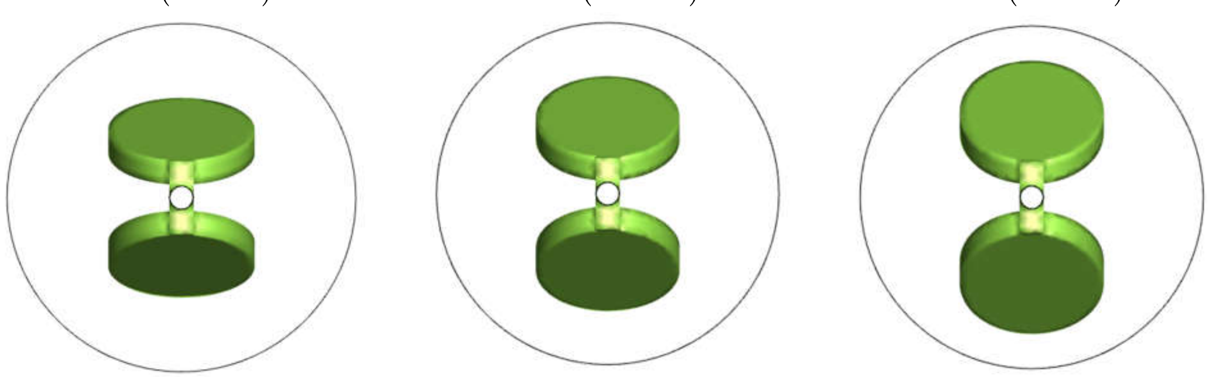

LS $\left(\theta = 15^{\circ}\right)$ LS $\left(\theta = 20^{\circ}\right)$ LS $\left(\theta = 25^{\circ}\right)$

b) Geometries of louvered strip inserts

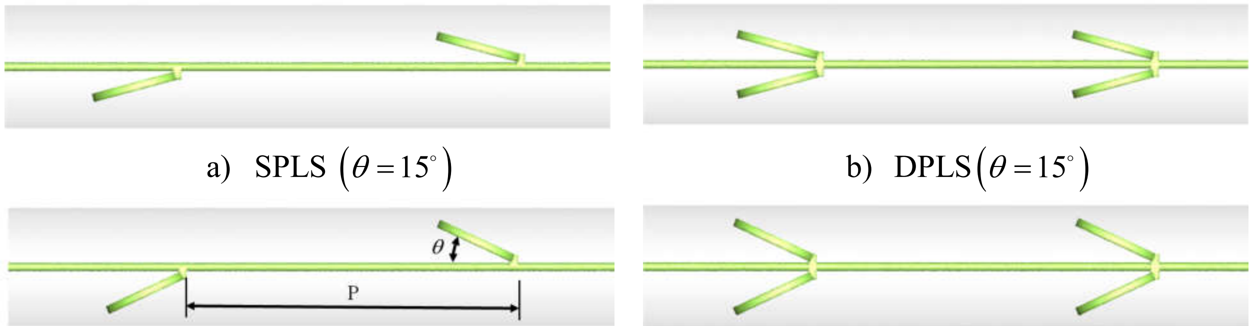

a) SPLS $(\theta = 15^{\circ})$ b) DPLS $(\theta = 15^{\circ})$

c) SPLS $(\theta = 25^{\circ})$ d) DPLS $(\theta = 25^{\circ})$

c) Position of perforated louvered strip inserts

Fig. 1 Schematic views of the heat exchanger pipe enhanced with perforated louvered strips with various geometries

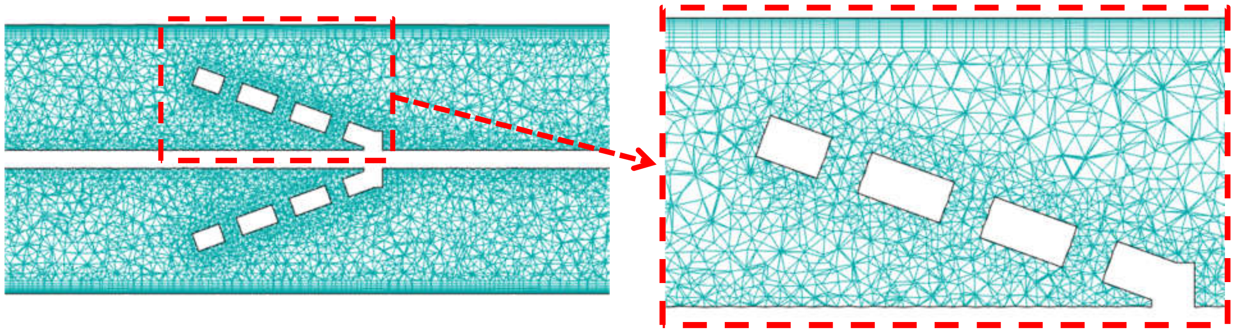

a) Side view

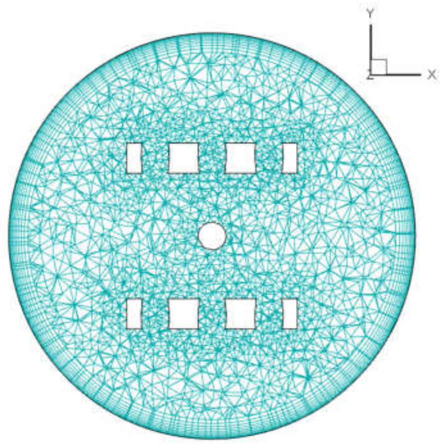

b) Front view

Fig. 2 Grid generation inside heat exchangers promoted with DPLS inserts

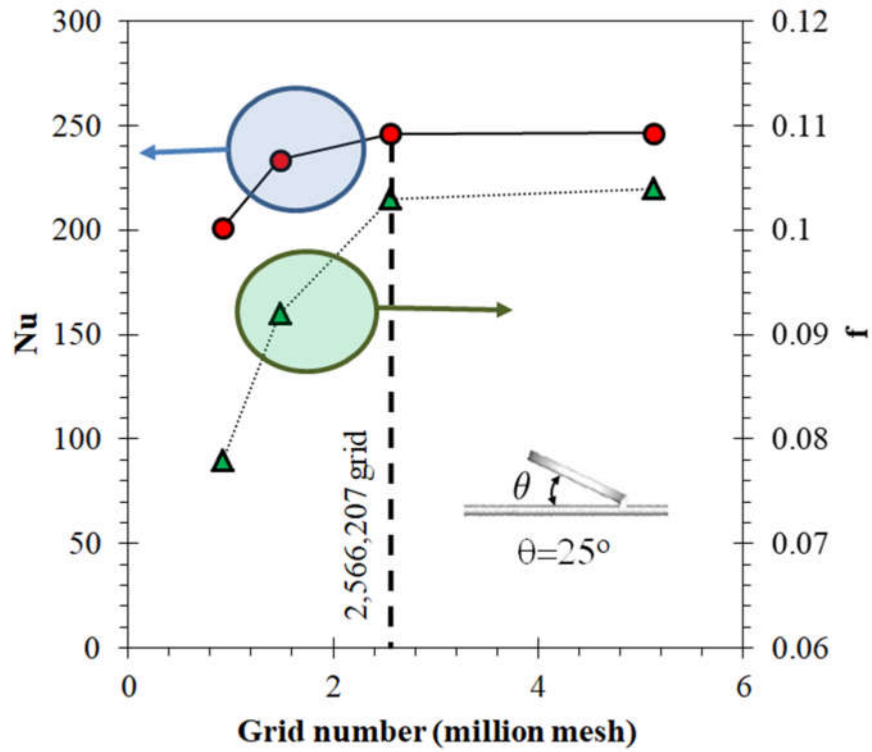

Fig. 3 Grid independency study for friction factor and Nusselt number for DPLS insert $\left(\theta = 25^{\circ}\right)$ at Re=14,000

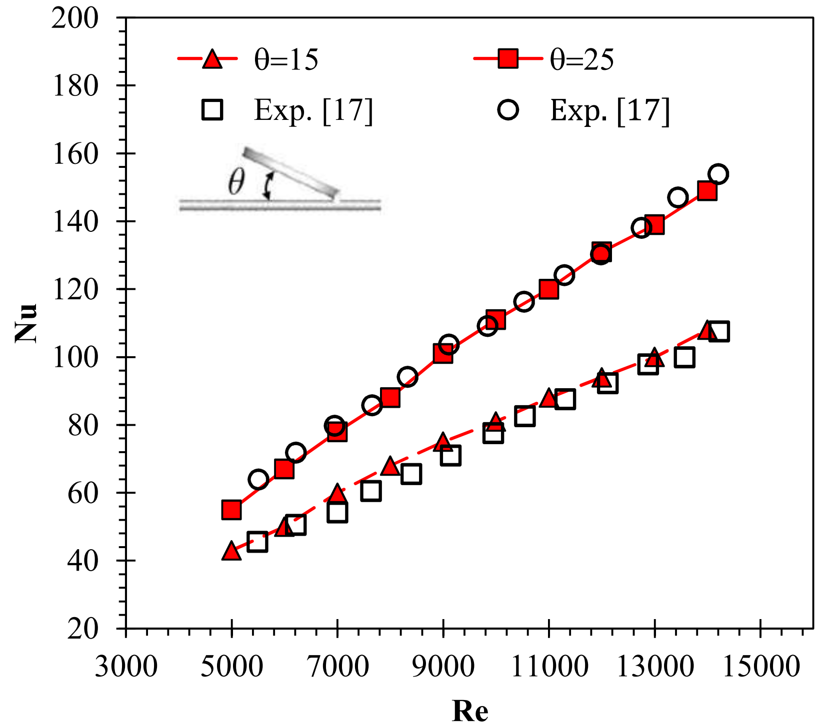

a) Nusselt number vs. Reynolds number

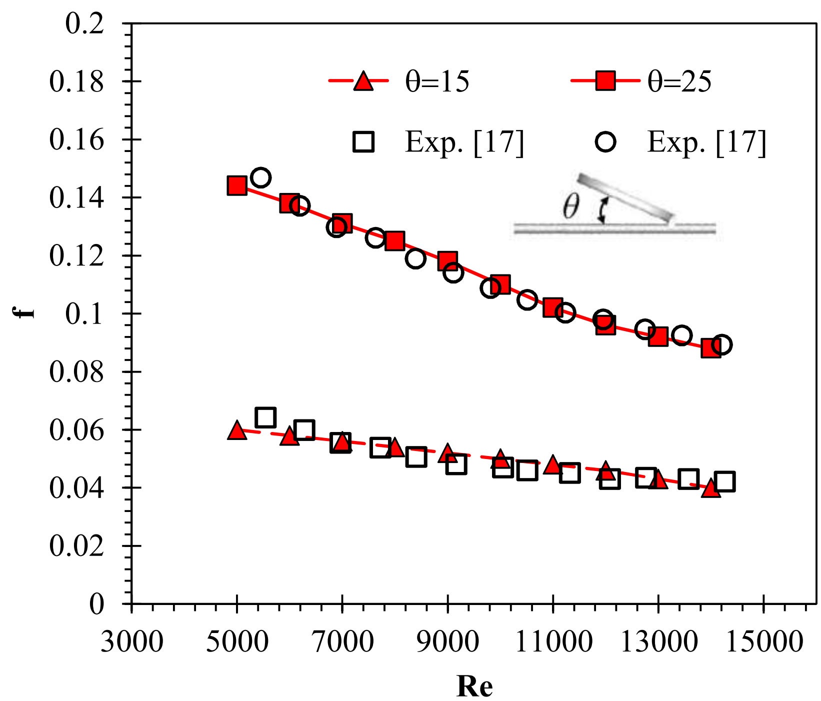

b) Friction factor vs. Reynolds number

Fig. 4 Validity of numerical simulations with experimental data [17]

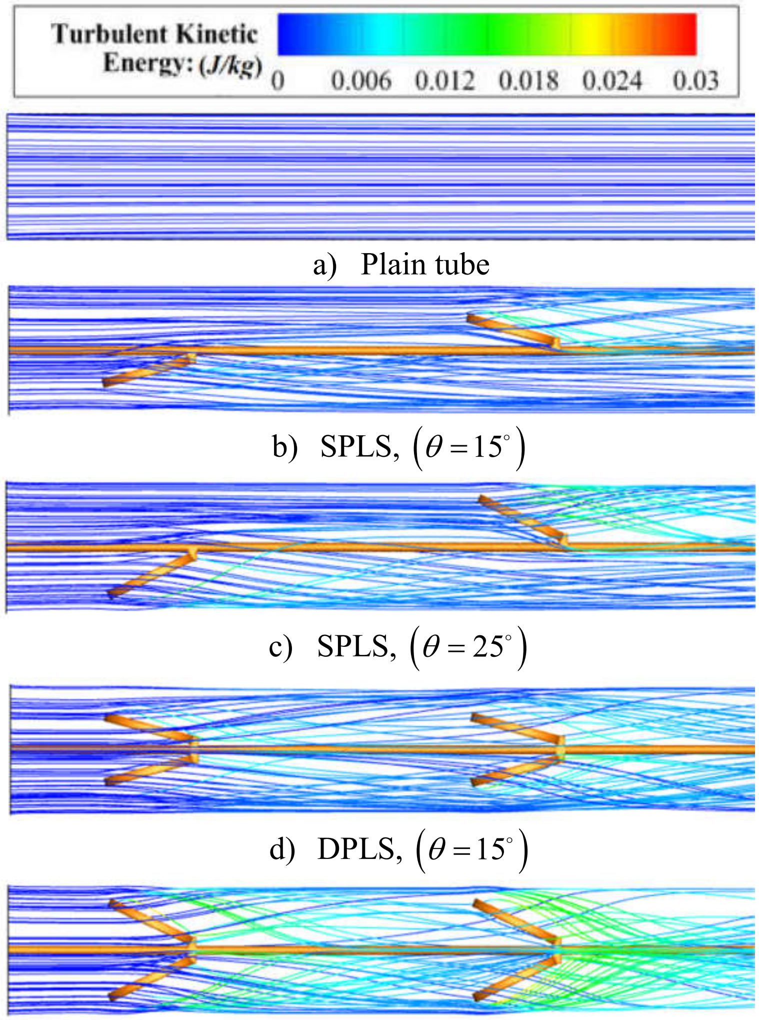

a) Plain tube

b) SPLS, $(\theta = 15^{\circ})$

c) SPLS, $(\theta = 25^{\circ})$

d) DPLS, $(\theta = 15^{\circ})$

e) DPLS, $(\theta = 25^{\circ})$

Fig. 5 TKE streamlines of nanofluid flow $(\phi = 1\%)$ through tubes fitted various PLS and DPLS inserts at Re=5,000.

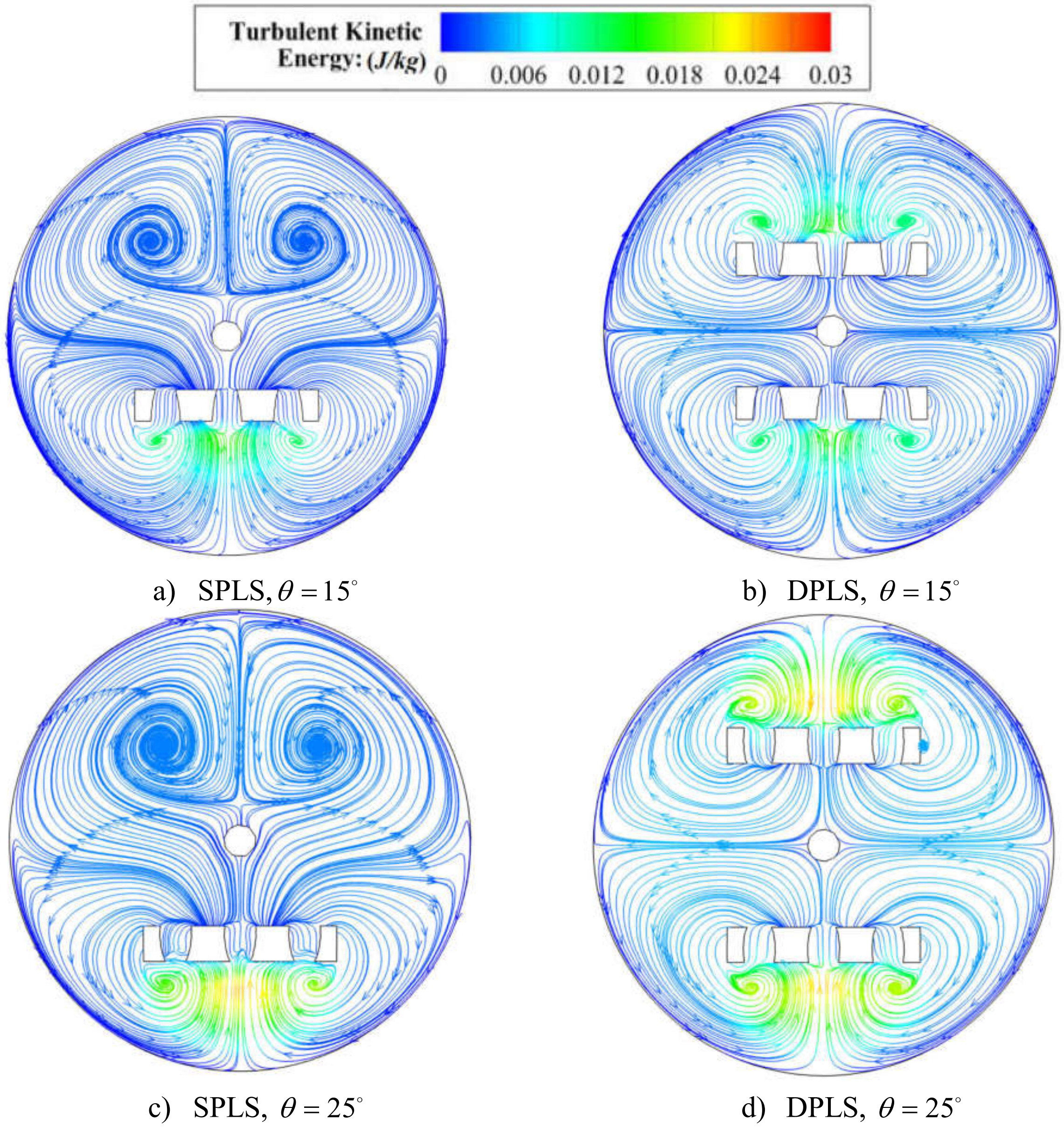

Fig. 6 Cross-section view of TKE surface streamlines of CuO-water nanofluids flow through heat exchanger tubes promoted by PLS and DPLS inserts

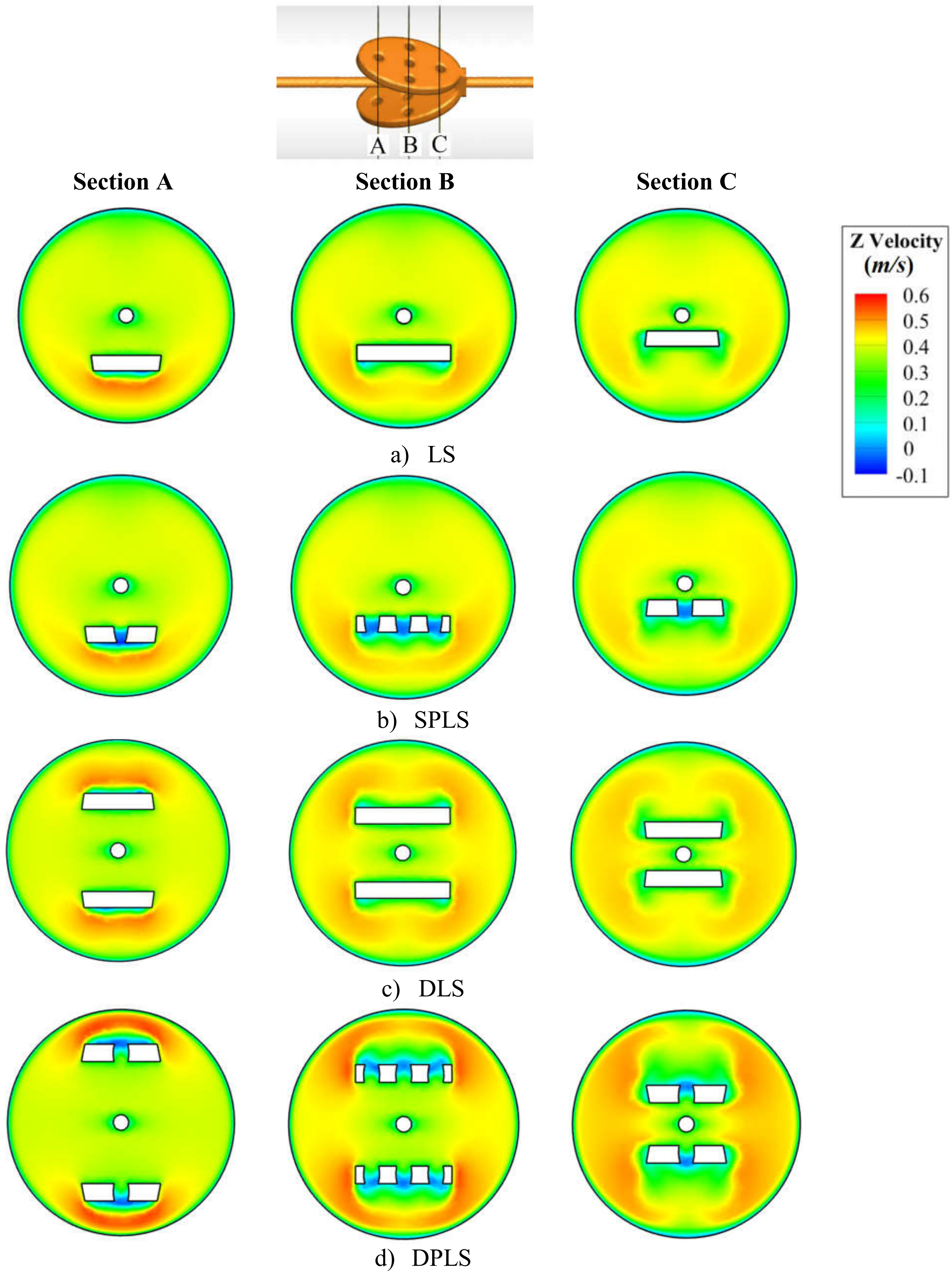
A
B
C
Section A
Section B
Section C
Z Velocity
(m/s)
0.6
0.5
0.4
0.3
0.2
0.1
0
-0.1
a) LS
b) SPLS
c) DLS
d) DPLS

Fig. 7 Axial velocity contours of turbulent nanofluids flow $(\phi = 1\%)$ near various louvered strip geometries at Re=5,000.

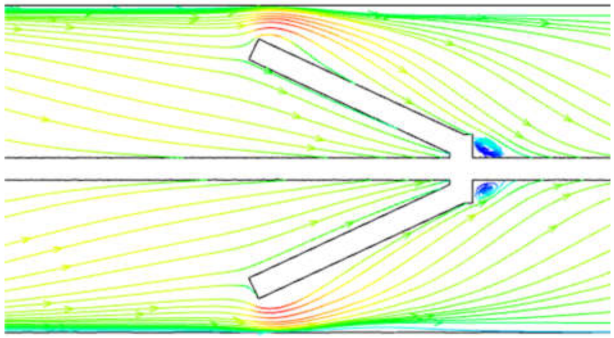

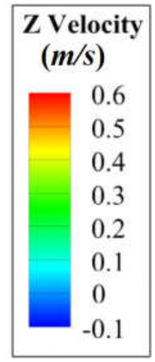

a) Typical louvered strip, $\left(\theta = 25^{\circ}\right)$

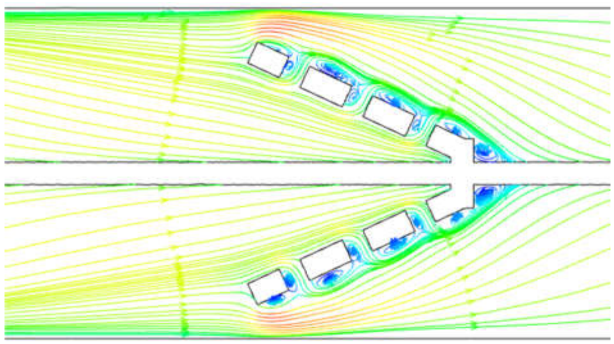

b) DPLS, $\left(\theta = 25^{\circ}\right)$

Fig. 8 surface streamlines of axial velocity near the typical louvered strip and DPLS inserts

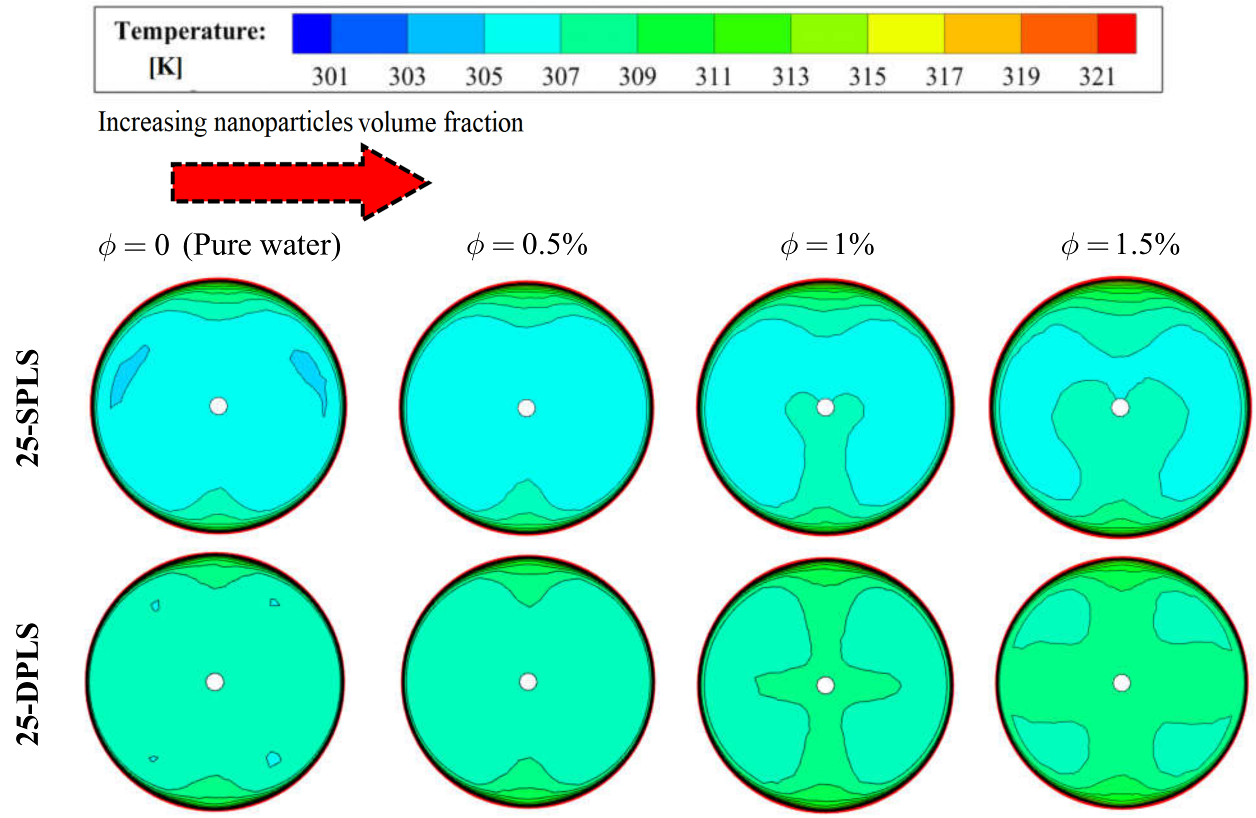

Fig. 9 Effects of nanoparticles volume fraction (ϕ) on the temperature distribution of nanofluid flow inside tubes fitted with SLPS and DPLS inserts.

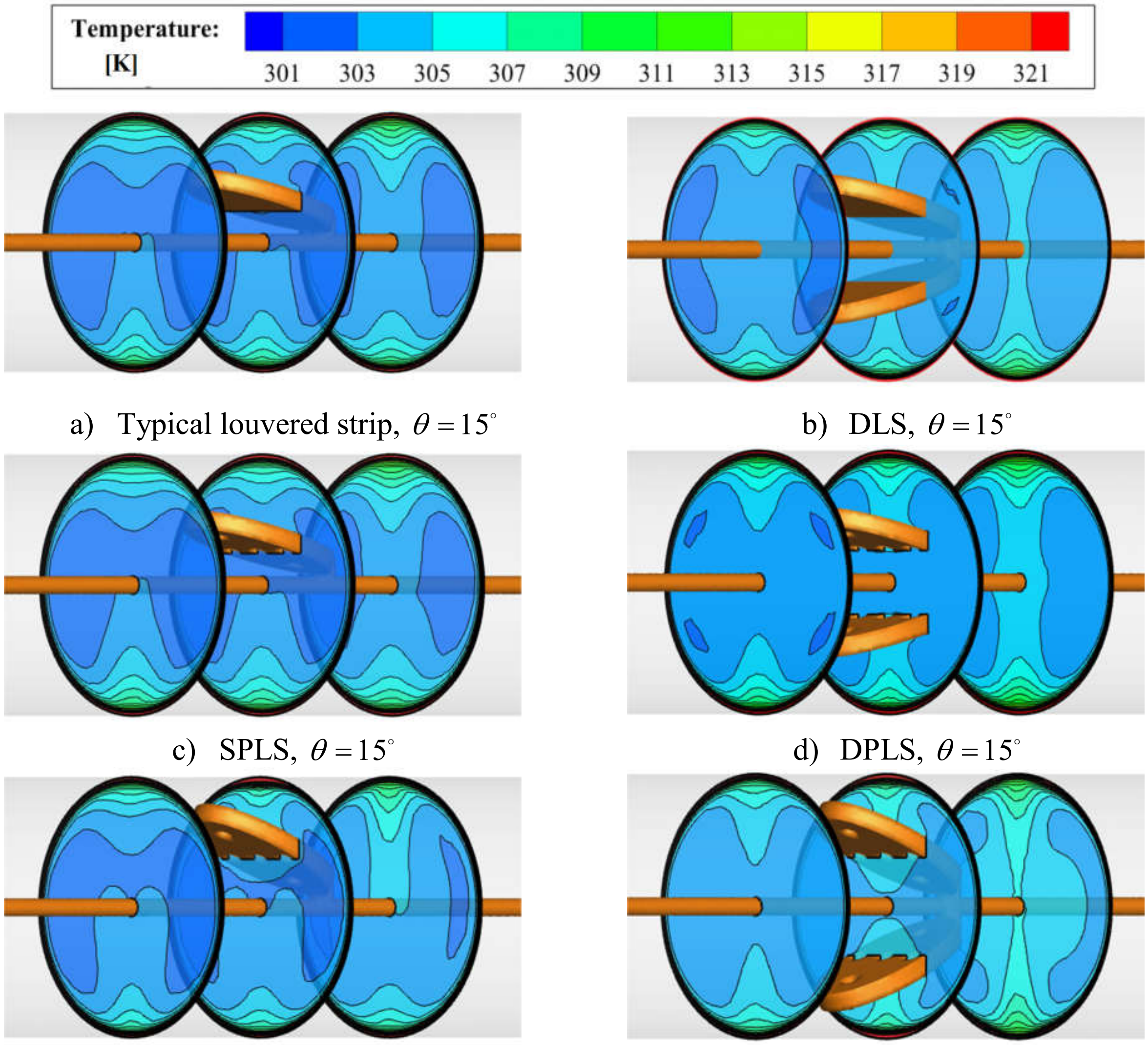

a) Typical louvered strip, $\theta = 15^{\circ}$ b) DLS, $\theta = 15^{\circ}$

c) SPLS, $\theta = 15^{\circ}$ d) DPLS, $\theta = 15^{\circ}$

e) SPLS, $\theta = 25^{\circ}$ f) DPLS, $\theta = 25^{\circ}$

Fig. 10 Temperature contours of nanofluids flow through heat exchanger pipes equipped by various louvered strip turbulators

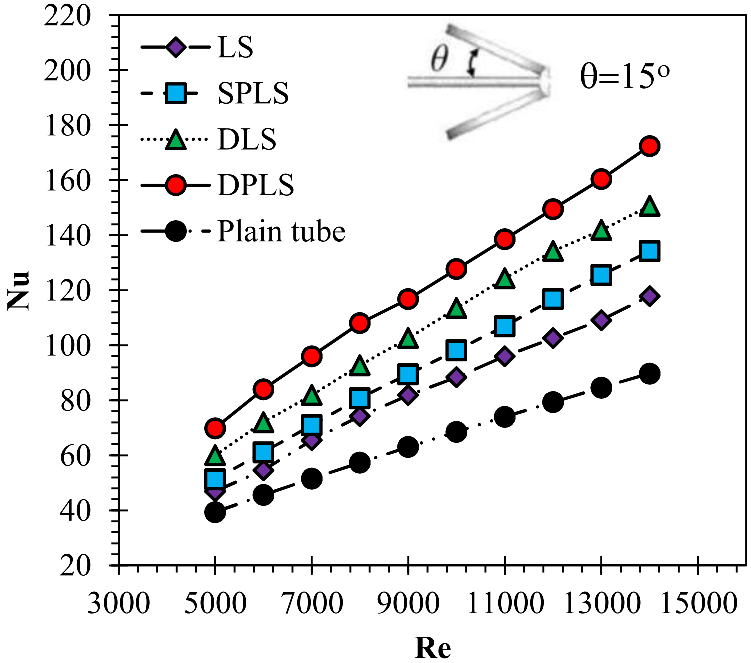

a) $\theta = 15^{\circ}$

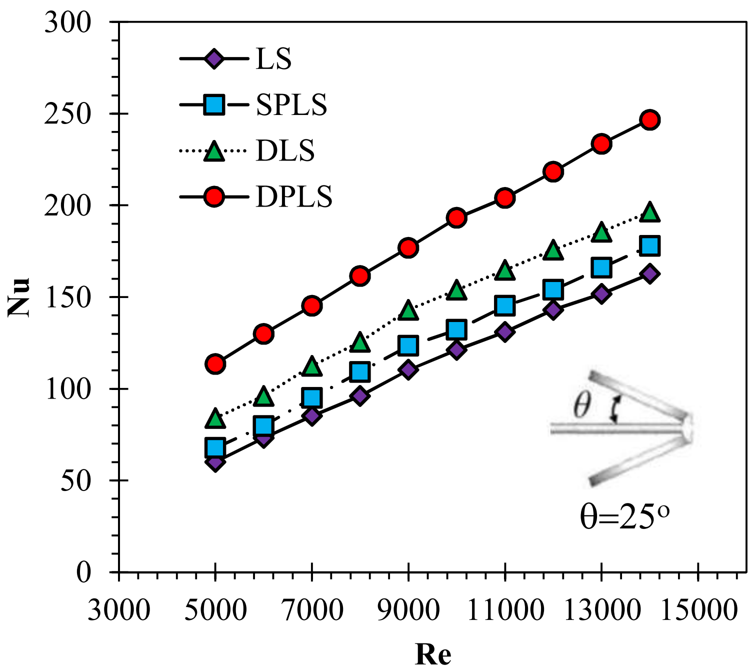

b) $\theta = 25^{\circ}$

Fig. 11 The effects of louvered strip geometry on the heat transfer coefficient of CuO-water nanofluid flow inside heat exchangers with various inclination angles.

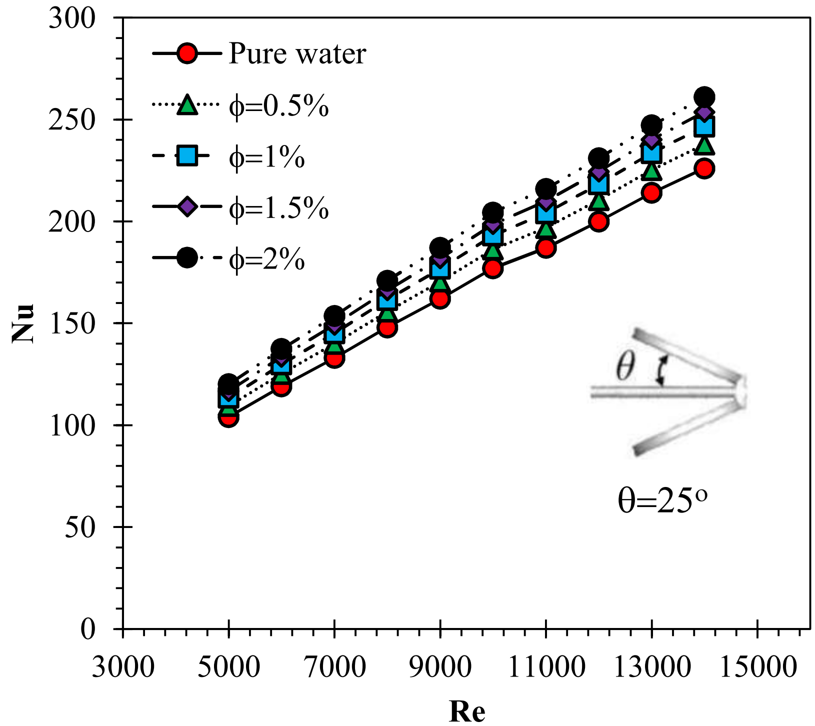

Fig. 12 The effect of CuO nano additive volume fraction (ϕ) on heat transfer enhancement inside heat exchanger tubes promoted by DPLS insert with $\theta = 25^{\circ}$

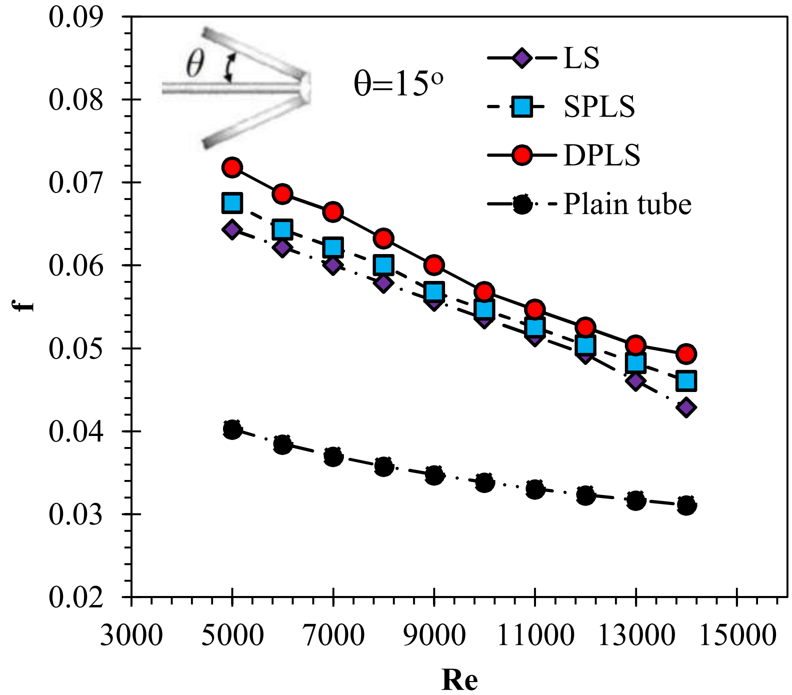

a) $\theta = 15^{\circ}$

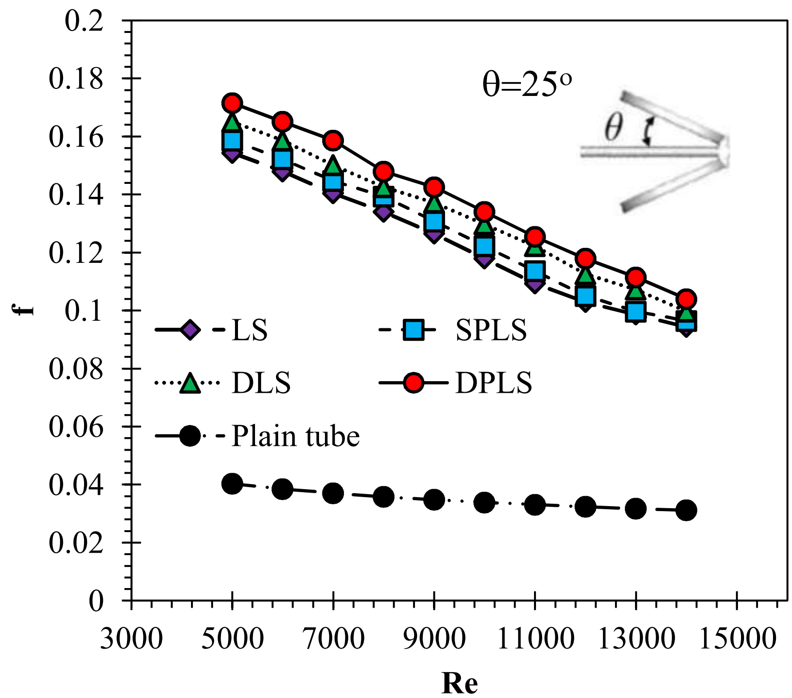

b) $\theta = 25^{\circ}$

Fig. 13 Variations of friction factor with the Reynolds number for heat exchanger pipes promoted by various louvered strips

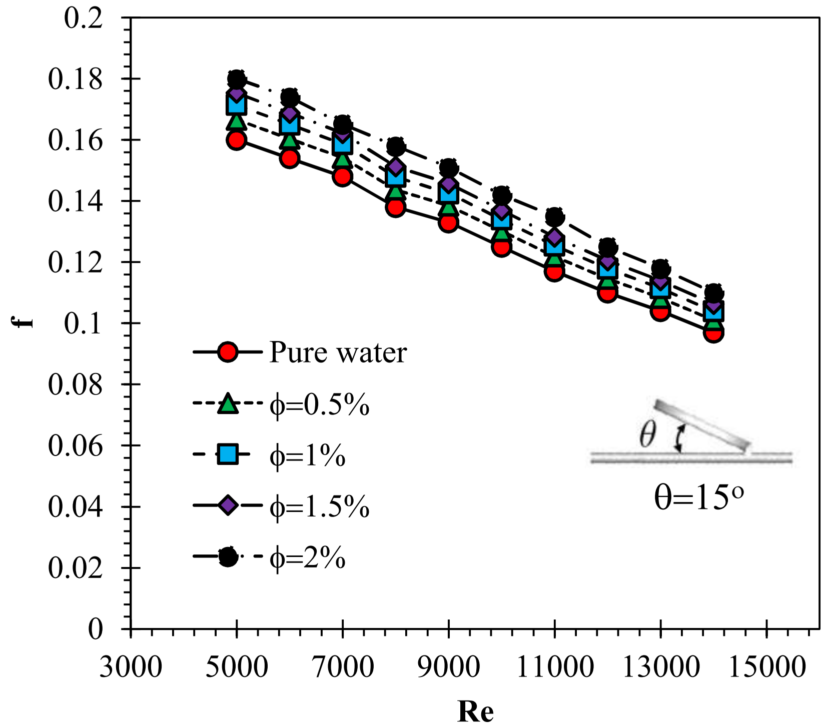

Fig. 14 The effects of nanoparticles volume concentration on the friction factor within heat exchangers equipped by DPLS turbulator with $\theta = 25^{\circ}$

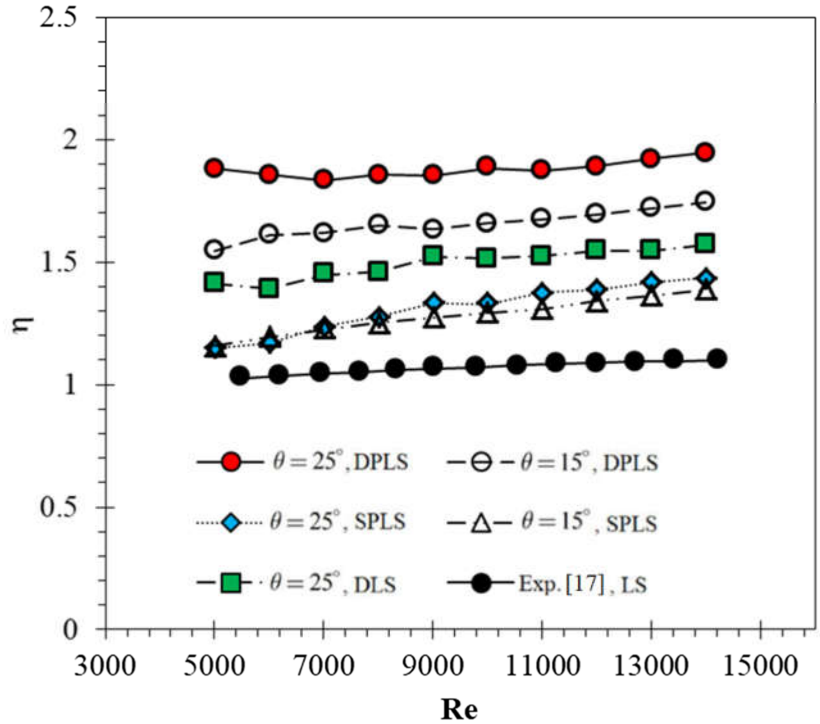

Fig. 15 Variations of thermal performance factor with respect to the Reynolds number for various louvered strip turbulators by varying inclination angles at $\phi = 2\%$.

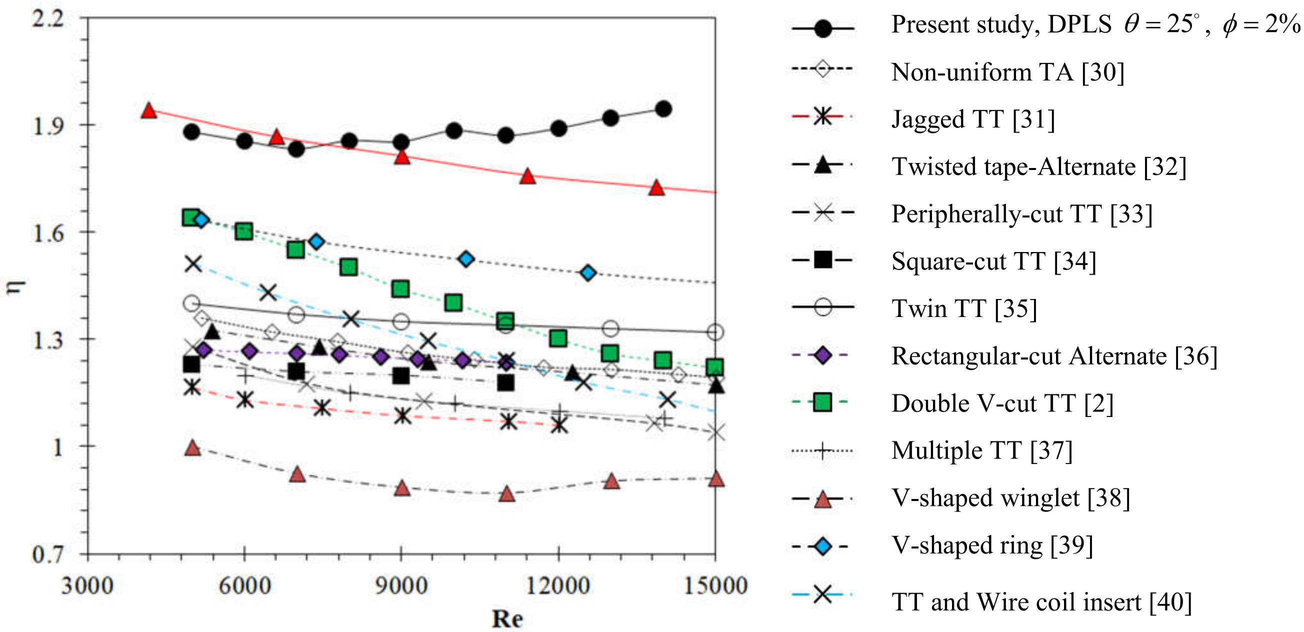

Fig. 16 Comparison between the thermal performance of the present study with recent studies in the field of vortex generators

List of Tables

Table 1 Validity of numerical simulations with experimental data for average Nu number of CuO-water nanofluid flow

Re	$\phi = 0.1\%$		$\phi = 0.3\%$	
	Present study	Exp. [29]	Present study	Exp. [29]
6205	55.69	56.88	57.82	58.61
7973	69.15	69.74	71.35	72.04
10117	78.23	80.00	87.92	85.79
13456	100.67	102.03	115.41	112.20